Androgen Action *via* the Androgen Receptor in Neurons Within the Brain Positively Regulates Muscle Mass in Male Mice

Rachel A. Davey,[1] Michele V. Clarke,[1] Patricia K. Russell,[1] Kesha Rana,[1] Jane Seto,[2] Kelly N. Roeszler,[2] Jackie M.Y. How,[1] Ling Yeong Chia,[1] Kathryn North,[2] and Jeffrey D. Zajac[1]

[1]Department of Medicine, Austin Health, University of Melbourne, Heidelberg, Victoria 3084, Australia; and [2]Murdoch Children's Research Institute, Parkville 3052, Victoria, Australia

Although it is well established that exogenous androgens have anabolic effects on skeletal muscle mass in humans and mice, data from muscle-specific androgen receptor (AR) knockout (ARKO) mice indicate that myocytic expression of the AR is dispensable for hind-limb muscle mass accrual in males. To identify possible indirect actions of androgens *via* the AR in neurons to regulate muscle, we generated neuron-ARKO mice in which the dominant DNA binding–dependent actions of the AR are deleted in neurons of the cortex, forebrain, hypothalamus, and olfactory bulb. Serum testosterone and luteinizing hormone levels were elevated twofold in neuron-ARKO males compared with wild-type littermates due to disruption of negative feedback to the hypothalamic-pituitary-gonadal axis. Despite this increase in serum testosterone levels, which was expected to increase muscle mass, the mass of the mixed-fiber gastrocnemius (Gast) and the fast-twitch fiber extensor digitorum longus hind-limb muscles was decreased by 10% in neuron-ARKOs at 12 weeks of age, whereas muscle strength and fatigue of the Gast were unaffected. The mass of the soleus muscle, however, which consists of a high proportion of slow-twitch fibers, was unaffected in neuron-ARKOs, demonstrating a stimulatory action of androgens *via* the AR in neurons to increase the mass of fast-twitch hind-limb muscles. Furthermore, neuron-ARKOs displayed reductions in voluntary and involuntary physical activity by up to 60%. These data provide evidence for a role of androgens *via* the AR in neurons to positively regulate fast-twitch hind-limb muscle mass and physical activity in male mice. (***Endocrinology*** **158: 3684–3695, 2017)**

It is well established that hypogonadism in men results in decreased lean mass (1). We and others showed that testosterone suppression in either men with prostate cancer or normal men causes a reduction in muscle size and strength (2, 3). Conversely, testosterone treatment increases muscle mass and strength, not only in hypogonadal men (4), but also in men with normal androgen levels (5). Androgens are not widely used to increase skeletal muscle mass and strength, however, not because of the lack of effect, but because of undesirable side effects (6). Therefore, a better understanding of the mechanisms by which androgens influence muscle growth and strength is essential to be able to better harness their therapeutic potential.

We and others have provided important insight into the mechanism by which androgens act to regulate the musculoskeletal system by generation of genetically modified mouse models in which the androgen receptor (AR) has been deleted either globally or in a tissue- and/or cell-specific manner using the Cre/loxP system. We have previously generated global-AR knockout (ARKO) mice that contain an in-frame deletion of exon 3 of the AR gene, which encodes the second zinc finger of the DNA binding domain of the AR (global-ARKO;$AR^{\Delta ZF2}$). This leads to the production of a mutant AR protein that

ISSN Print 0013-7227 ISSN Online 1945-7170
Printed in USA
Copyright © 2017 Endocrine Society
Received 16 May 2017. Accepted 25 July 2017.
First Published Online 31 July 2017

Abbreviations: AR, androgen receptor; ARKO, androgen receptor knockout; CaMKIIα, calcium/calmodulin-dependent protein kinase IIα; cDNA, complementary DNA; EDL, extensor digitorum longus; Gast, gastrocnemius; IGF-1, insulinlike growth factor-1; LA, levator ani; LH, luteinizing hormone; mRNA, messenger RNA; PBS, phosphate-buffered saline; PCR, polymerase chain reaction; Sol, soleus; WT, wild-type.

Downloaded from https://academic.oup.com/endo/article-abstract/158/10/3684/4056265 by Biomedical Library user on 04 April 2019

cannot signal through the dominant DNA-binding dependent pathway, whereas the non-DNA binding-dependent actions of the AR remain functional (7, 8). Data from our global-ARKOs demonstrate that the AR is required for development of normal muscle mass and strength in males (9). Hind-limb muscle mass is decreased by up to 20% in global-ARKOs compared with wild-type (WT) males with the fast-twitch extensor digitorum longus (EDL) muscle of global-ARKOs having reduced contractile strength, whereas the slow-twitch soleus (Sol) muscle has increased resistance to fatigue (9). Similar findings have been reported in an AR-null male mouse model generated by breeding exon 2–floxed AR mice with PGK-Cre mice, resulting in a frame shift mutation and the absence of AR protein. AR-null mice exhibit reductions in the weight and fiber cross-sectional area of the quadriceps muscle (10). In contrast, a different AR-null mouse model generated by breeding exon 2–floxed AR mice with β-actin–Cre mice displayed a decrease in the expression of fast-twitch and an increase in the expression of slow-twitch specific skeletal muscle proteins in the quadriceps muscle compared with WT controls in the absence of any histological differences being observed (11). It is possible that the mixed genetic background of the latter AR-null mouse line may account for the lack of effect observed on the morphology of the quadriceps muscle in these mice. In contrast to these findings of reduced hind-limb mass in global-ARKO and AR-null mouse models (9, 10), a number of mouse models in which either exon 1, 2, or 3 of the AR has been deleted specifically in cells of the muscle lineage in male mice, including satellite cells, myocytes, myoblasts, and/or myofibers, failed to demonstrate any effect on hind-limb muscle mass (12–14). With respect to muscle function, however, deletion of exon 2 of the AR specifically in satellite cells, myoblast, myocytes, and myofibers using MyoD-Cre mice (12) or deletion of exon 1 of the AR in both myoblasts and myocytes using HSA-Cre mice (14) results in a reduction in maximal grip strength of the hind-limb muscles. Although these data from the muscle-ARKOs support the notion that the expression of the AR in muscle cells is dispensable for hind-limb muscle mass, AR expression in the perineal muscles is essential for their development as the mass of the levator ani (LA) was markedly reduced in all muscle-ARKOs published to date (12–15). Together these data indicate that, although AR expression in hind-limb muscle is essential for maximum peak force production, it is not required for peak muscle mass, suggesting the major target of androgen action to regulate hind-limb muscle mass is mediated *via* the AR in another target tissue.

One possible mechanism by which androgens may regulate hind-limb muscle mass is *via* the AR in the central nervous system. Although few studies have investigated the central regulation of skeletal muscle mass, there is some evidence that suggests that central regulation occurs, with studies showing that pulsatile growth hormone secretion regulates muscle mass (16), and central administration of an interleukin-1 receptor antagonist can block sepsis-induced loss of muscle mass and inhibition of protein synthesis (17). To date, two neuron-ARKO mouse models have been generated by mating exon 2–floxed AR mice with either Nestin-Cre (18) or Synapsin-Cre mice (19). Unfortunately, limited insight into the role of the AR in neurons to regulate skeletal muscle mass can be gained from these neuron-ARKO models. The neuron-ARKOs generated using the Nestin-Cre mice did not exhibit any changes in muscle, fat, or bone mass compared with littermate control mice when corrected for their lower body weight (18). The phenotype of these neuron-ARKOs, however, is likely to be attributed to the metabolic phenotype of the Nestin-Cre mice. Nestin-Cre mice exhibit reduced body length, mild hypopituitarism, reduced serum growth hormone levels, together with improved insulin sensitivity due to the unexpected expression of human growth hormone in the hypothalamus (20, 21). In the neuron-ARKO mice generated using Synapsin-Cre mice, hind-limb muscle mass was not analyzed. These mice did exhibit hepatic insulin resistance leading to lipid accumulation and visceral obesity (19); however, it should be noted that Cre is also expressed in the testes of Synapsin-Cre mice, leading to marked germline deletion of the target gene (20).

We propose that the anabolic actions of androgens on hind-limb muscle mass are mediated, at least in part, indirectly *via* the AR in neurons. To test this hypothesis and to overcome the limitations of the previous neuron-ARKO models, we have generated a genetically modified mouse model in which the dominant DNA binding–dependent (genomic) actions of the AR are deleted specifically in neurons within the brain (neuron-ARKOs) using calcium/calmodulin-dependent protein kinase IIα (CamIIKα)–iCre mice (22). Unlike the Nestin-Cre (18) and Synapsin-Cre (19) mice, target gene deletion mediated by the mouse CaMKIIα promoter has been shown to be highly specific for neurones (22). The aim of the current study was to determine the contribution of androgens acting *via* the AR in neurons in the regulation of muscle development, mass, and function.

Materials and Methods

Generation of neuron-ARKO mice

Neuron-AR$^{\Delta ZF2}$ mice with an in-frame deletion of exon 3 of the AR, which encodes the second zinc finger of the DNA binding domain, were generated by breeding heterozygous

Downloaded from https://academic.oup.com/endo/article-abstract/158/10/3684/4056265 by Biomedical Library user on 04 April 2019

female floxed AR mice lacking the neomycin selection cassette ($AR^{loxP(neo-)/WT}$) (7, 23) with male mice in which iCre expression is under the control of the mouse CaMKIIα promoter expressed shortly after birth (postnatal day 20) (CamKIIα-iCre$^{+/-}$) (22, 24). These mice will be referred to as neuron-ARKOs for simplicity. All genetically modified mouse lines were on a congenic C57BL/6J background. As the wet weights of the androgen-dependent organs seminal vesicles, testes, kidneys, subcutaneous fat, and the highly androgen-dependent pelvic muscle, the LA, in addition to the hind-limb muscles [gastrocnemius (Gast), Sol, and EDL] of male $AR^{loxP(neo-)/Y}$ and male CaMKII-iCre mice did not differ from male WT littermate controls (Supplemental Table 1) (23), all comparisons were performed using WT littermates as controls. Mice were housed in a specified pathogen-free facility at 22°C in a 12-hour light/12-hour dark cycle and were supplied with standard irradiated mouse chow (1.2% calcium, 0.96% phosphorus; Ridley Agriproducts, Corowa, NSW, Australia) and water *ad libitum*. For food intake measurements, mice at 12 weeks of age were housed individually and measured at the beginning and end of a 5-day period and averaged for daily intake. All procedures were approved by the Austin Health Animal Ethics Committee and complied with the Australian Code of Practice for the Care and Use of Animals for Scientific Purposes.

Genotyping

Genomic DNA isolated from tail biopsy was used as a template for polymerase chain reaction (PCR) genotyping. The floxed AR genotyping protocol has been described previously (23). The primer pair sequences used for identifying the CAMKIIα-iCre transgene are as follows: CAMKIIα-iCre coding sequence forward, 5′-GGTTCTCCGTTTGCACTCAGGA-3′; reverse, 5′-CCTGTTGTTCAGCTTGCACCAG-3′. Template was 100 ng genomic DNA amplified in the presence of 0.25 nM each primer, 1.5 mM $MgCl_2$, and 0.25 nM dNTPs in a 20 μL reaction volume. Cycling conditions are as follows: initial denaturation step of 95°C for 5 minutes, followed by 35 cycles of denaturation at 95°C for 30 seconds, annealing at 54°C for 30 seconds, and extension at 72°C for 1 minute.

Physical activity

Voluntary activity was measured at 6 and 12 weeks of age by monitoring the use of running wheels with a computerized meter, as previously described (25). Mice were individually housed for 7 days in boxes containing a 15-cm–diameter running wheel and had access to water and food *ad libitum*. The initial 2 days were allowed for acclimatization, and readings were recorded over the 5 days following acclimatization. These recordings were averaged and expressed as counts/day. Involuntary physical activity (spontaneous activity) was measured at 6 and 12 weeks of age in individually housed mice that had free access to food and water using an infrared light beam monitor (Columbus Instruments, Columbus, OH). Mice were allowed 24 hours of acclimatization to the activity meters, after which measurements were taken every 24 hours for 2 days, averaged, and expressed as counts/day.

Tissue collection and serum analyses

WT and neuron-ARKO mice were euthanized at 6 and 12 weeks of age by lethal intraperitoneal injection of ketamine (110 mg/kg body weight) and xylazine (20 mg/kg body weight), following an overnight fast in 12-week-old mice. Body weights were recorded, and cardiac blood was collected from 12-week-old mice for hormone analyses. Following euthanasia, tissues were immediately excised, weighed, frozen in liquid nitrogen, and stored at −80°C. The hind-limb muscles Gast, EDL, and Sol; the perineal muscle LA; and seminal vesicles, testes, kidneys, heart, spleen, and fat pads were excised, and wet weight was determined to an accuracy of 0.1 mg. The brain was collected and dissected into seven regions (brainstem, cerebellum, cortex, forebrain, hypothalamus, olfactory bulb, and pituitary) using a mouse brain matrix and stored at −80°C.

Serum hormone analyses were performed on sera collected from WT and neuron-ARKOs at 12 weeks of age. Serum testosterone levels were determined, as previously described (26). Briefly, serum was organically extracted with hexane-ethyl acetate (17:3) in silanized glass tubes prior to analysis by enzyme-linked immunosorbent assay (Abcam, Melbourne, Victoria, Australia), according to the manufacturers' instructions. Luteinizing hormone (LH; MyBioSource, San Diego, CA) and insulinlike growth factor-1 (IGF-1; Abcam, Cambridge, UK) were determined by enzyme-linked immunosorbent assay.

RNA extraction, complementary DNA synthesis, and reverse transcription PCR

Total RNA was isolated from the hypothalamus, pituitary, forebrain, kidney, testes, gonadal fat, heart, tibia, and Gast muscle of neuron-ARKOs and WT controls at 6 weeks of age, as described previously (27). Total RNA (5 μg) was treated with 5 U DNase I (DNA-Free Kit; Ambion, Scoresby, Victoria, Australia), according to the manufacturers' instructions. Complementary DNA (cDNA) was synthesized from 1 μg DNase-treated RNA using random hexamers (Promega, Madison, WI) and Moloney murine leukemia virus reverse transcription, according to the manufacturers' instructions (Promega). The resulting cDNA was subjected to PCR with the AR-specific primers that flank exon 3, as follows: exon 2 forward primer, 5′-GACAGTACCAGGGACCATGTT-3′ and exon 4 reverse primer, 5′-CTCAATGGC TTCCAGGACGTT-3′. PCR was performed for 35 cycles at 94°C for 30 seconds, 54°C for 30 seconds, and 72°C for 45 seconds.

Quantitative real-time PCR

Total RNA was isolated and cDNA was synthesized from Gast and seven different regions of the brain representing the cerebellum, cortex, forebrain, hypothalamus, olfactory bulb, pituitary, and peripheral nerves (located between L3 and L5), as described previously (27). To determine total AR messenger RNA (mRNA) levels in the different brain regions of neuron-ARKOs, quantitative real-time PCR was performed in duplicate using 50 ng cDNA per 20 μl reaction on an Applied Biosystems 7500 real-time PCR system using an AR (exon 3-specific) Applied Biosystems TaqMan gene expression assay (assay identification: Mm00442688; Applied Biosystems, Foster City, CA). The mRNA levels of Igf1 (assay identification: Mm00439561_m1), transforming growth factor β1 (*Tgfβ1*; assay identification: Mm00441724_m1), and a number of muscle-specific genes, including myosin light chain 3 (*Myl3*; assay identification: Mm00803034_m1), myosin heavy chain 7 (*MyH7*; assay identification: Mm00600555_m1), troponin I2 (*TnnI2*; assay identification: Mm01290256_m1), myogenic

Downloaded from https://academic.oup.com/endo/article-abstract/158/10/3684/4056265 by Biomedical Library user on 04 April 2019

differentiation 1 (*Myod1*; assay identification: Mm00440387_m1), and myosin heavy chain 4 (*MyH4*; assay identification: Mm01332541_m1), were determined in Gast muscle of WT and neuron-ARKOs. Absolute expression was calculated using the $\Delta\Delta C_T$ method, with the gene of interest normalized to a housekeeping gene chosen for each tissue of interest based on their documented stability of expression and expressed relative to a reference sample. Housekeeping genes used are as follows: phosphoglycerate kinase 1 (*Pgk1*; assay identification: Mm00435617) (28) for brain samples and eukaryotic translation elongation factor 2 (*Eef2*; assay identification: Mm00833287_g1) (29) for muscle samples.

Muscle fiber-typing analyses

Gast muscles were bisected across the midsection and mounted in optimal cutting temperature medium. Transverse 8-μm–thick sections were blocked in 2% bovine serum albumin for 10 minutes and immunostained with an antibody specific to MyHC 2B (BF-F3; Developmental Studies Hybridoma Bank, Iowa City, IA) (Table 1) overnight at 4°C in a lightproof, humidified chamber. Sections were then washed in 1× phosphate-buffered saline (PBS) three times for 5 minutes and reblocked in 2% bovine serum albumin, and then incubated with A594-immunoglobulin M goat anti-mouse secondary (Table 1) for 1 hour at room temperature. After PBS washing, sections were incubated with A488-labeled wheat germ agglutinin (Molecular Devices, Sunnyvale, CA) to demarcate fiber borders. Sections were then washed in PBS, fixed in 4% paraformaldehyde for 10 minutes, and then mounted with Immu-mount (Thermo Scientific, Waltham, MA). Slides were imaged using a Leica microscope (Wetzlar, Germany) and Metaviewer software (Metasystems, Altlusheim, Germany). Fiber analyses were performed using Metamorph software (Molecular Devices), as previously described (30).

Western blot analysis

Total cell lysate was extracted from Gast hind-limb muscle (n = 4 per group) in radioimmunoprecipitation assay buffer (PBS, 1% Nonidet P-40, 0.5% sodium deoxycholate, and 0.1% sodium dodecyl sulfate) with protease inhibitors (Complete; Roche, Basel, Switzerland). A total of 30 μg extracted protein was loaded on a 10% reducing sodium dodecyl sulfate–polyacrylamide gel electrophoresis. The gel was transferred onto 0.2 μm polyvinylidene difluoride membrane (ImmunBlot; Bio-Rad, Hercules, CA). Blots were blocked in 3% milk/PBS/0.05% Tween 20, and then incubated with total oxidative phosphorylation rodent Western blot antibody cocktail (ab110413; Abcam, Cambridge, UK) (Table 1) diluted 1:2000 in 5% milk/PBS/0.05% Tween. Blots were then incubated with a horse anti-mouse immunoglobulin G conjugated to horseradish peroxidase secondary (Table 1) for 1 hour at room temperature (Cell Signaling Technology, Danvers, MA). Clarity Western ECL substrate (Bio-Rad, Hercules, CA) was used to visualize the blots on a Fujifilm LAS3000. The blots were stripped, blocked in 3% milk/PBS/0.05% Tween, and then reprobed with α-tubulin (AA4.3; Developmental Studies Hybridoma Bank) (Table 1) diluted 1:1000 in 1% milk/PBS Tween 20 overnight. The next morning, after washing, the blot was incubated for 1 hour in a 1:3000 dilution of goat anti-mouse immunoglobulin G–horseradish peroxidase (DAKO P0447, Santa Clara, CA) (Table 1) in 1% milk/PBS Tween 20 at

Table 1. Antibody Table

Peptide/Protein Target	Antigen Sequence (if Known)	Name of Antibody	Manufacturer, Catalog No.	Species Raised in; Monoclonal or Polyclonal	Dilution Used	RRID
Myosin heavy chain 2B		MyHC 2B	Developmental Studies Hybridoma Bank, BF-F3	Mouse; monoclonal	1:10	AB_2266724
Mouse IgM heavy chain		Alexa Fluor® 594 Goat anti-mouse IgM	Life Technologies, A21044	Goat anti-mouse; clonality unknown	1:200	AB_2535713
CI subunit NDUFB8 CII-30-kDa SDHB CIII-core protein 2 UQCRC2 CIV subunit I MTCO1 CV α subunit ATP5A		Total OXPHOS Rodent WB Antibody cocktail	Abcam, ab110413	Mouse; monoclonal	1:2000	AB_110242 AB_14714 AB_14745 AB_14705 AB_14748
Mouse IgG (light and heavy chain)		Anti-mouse IgG, HRP-linked antibody	Cell-Signaling Technology, 7076	Horse anti-mouse; polyclonal	1:2000	AB_330924
Mouse IgG, mouse IgM		Polyclonal goat anti-mouse immunoglobulins antibody	Dako	Goat; polyclonal antibody	1:3000	AB_2617137
α-Tubulin		Tubulin (α)	Developmental Studies Hybridoma Bank, AA4.3	Mouse; monoclonal	1:1000	AB_579793

Abbreviations: HRP, horseradish peroxidase; IgG, immunoglobulin G; IgM, immunoglobulin M; MTCO1, mitochondrially encoded cytochrome c oxidase I; NDUFB8, NADH deydrogenase [ubiquinone] 1 β subcomplex subunit 8, mitochondrial; OXPHOS, oxidative phosphorylation; RRID, Research Resource Identifier; SDHB, succinate dehydrogenase [ubiquinone] iron-sulfur subunit, mitochondrial; UQCRC2, ubiquinol-cytochrome c reductase core protein II; WB, Western blot.

Downloaded from https://academic.oup.com/endo/article-abstract/158/10/3684/4056265 by Biomedical Library user on 04 April 2019

room temperature and visualized, as described earlier. Densitometry analysis was performed using Multiguage software (Fulifilm, Fuji, Tokyo), and the protein levels of the five oxidative phosphorylation subunits were normalized to α-tubulin.

In situ muscle function analyses

In situ muscle function analyses of the Gast muscle were performed in WT and neuron-ARKOs at 10 weeks of age (n = 8 to 9 per group) using the Aurora Scientific 1300A whole-mouse test system and 701C stimulator (Ontario, ON, Canada). Mice were anesthetized using isofluorane (0.6 ml/min) and placed on a 37°C heated platform, and fur on the left hind-limb was removed by shaving. An incision was made in the skin to expose the Achilles tendon, the Gast muscle, and the knee. Surgical silk (silicon-coated suture silk 5/0; Covidien, Minneapolis, MN) was used to secure the Achilles tendon to the force transducer (model 809B *in situ* test apparatus), and the foot and knee were clamped in place for stability. Maximum tetanic force (mN) and specific force (mN/mm^2) were determined, as previously outlined in Banks *et al.* (31), with minor modifications. Briefly, the Gast muscle was adjusted to an optimum length (Lo) to produce maximal twitch force (Pt); fiber length (Lf) was derived from Lo after correcting for the pennation angle (Lf = Lo $\times$ 0.45). To generate force-frequency curves, the Gast was stimulated along the sciatic nerve every 2 minutes at increasing frequencies (5 to 250 Hz). To examine response to fatigue, muscles were allowed to rest for 5 minutes after the force-frequency test. Muscles were then repeatedly stimulated to fatigue at 150 Hz, 350 ms (1 second on, 1 second off) over 120 seconds, and force recovery was examined at 1, 2, 3, 5, and 10 minutes after fatigue. Results were presented as percentage of maximal force.

Statistical analyses

Comparisons between parameters measured in the littermate control groups (*i.e.*, WT, floxed AR, and CAMKIIα-iCre) were performed using a one-way analysis of variance with a Tukey or Tamhane *post hoc* test assuming equal or unequal variance, respectively, as indicated by Levene test for homogeneity of variance. Differences between WT and neuron-ARKO mice were identified using an unpaired Student *t* test with Levene test for homogeneity of variance. Force-frequency curves in WT and neuron-ARKOs were analyzed using a random-effects generalized least squares regression with individual animals as a random effect, percentage of force as a dependent variable, and genotype and time as independent variables. The interaction of time and genotype was also included in this model. All analyses were performed in IBM SPSS Statistics for Macintosh, Version 22 (New York, NY). A value of $P < 0.05$ was considered significant. Data are presented as mean $\pm$ standard error of the mean.

Results

Validation of neuron-ARKO mice

To investigate androgen signaling in neurons on skeletal muscle mass and function, we generated mice in which the genomic actions of the AR are selectively ablated in neurons within the brain (neuron-ARKOs). Recombination of the floxed AR allele, resulting in excision of exon 3 of the AR gene, was demonstrated by reverse transcription PCR analysis of cDNA extracted from the hypothalamus, pituitary, and forebrain of neuron-ARKOs (Fig. 1A). Importantly, the deleted AR allele was not detected in control tissues of neuron-ARKOs, namely gonadal fat, bone, or Gast muscle, with negligible levels of deletion observed in kidney, heart, and testes (Fig. 1A). Quantitative real-time PCR analyses in brain regions of the neuron-ARKOs determined that deletion of exon 3 of the AR was highly efficient, with AR exon 3 mRNA being undetectable in the cortex and olfactory bulb, decreased by >99% in the hypothalamus and forebrain, by 77% in the cerebellum, and by 35% in the pituitary, whereas it was not deleted in peripheral nerves (Fig. 1B).

Serum testosterone, LH, and follicle-stimulating hormone are elevated in neuron-ARKO mice

Serum testosterone was increased twofold in neuron-ARKOs at 12 weeks of age (Fig. 2A) ($P < 0.05$), leading

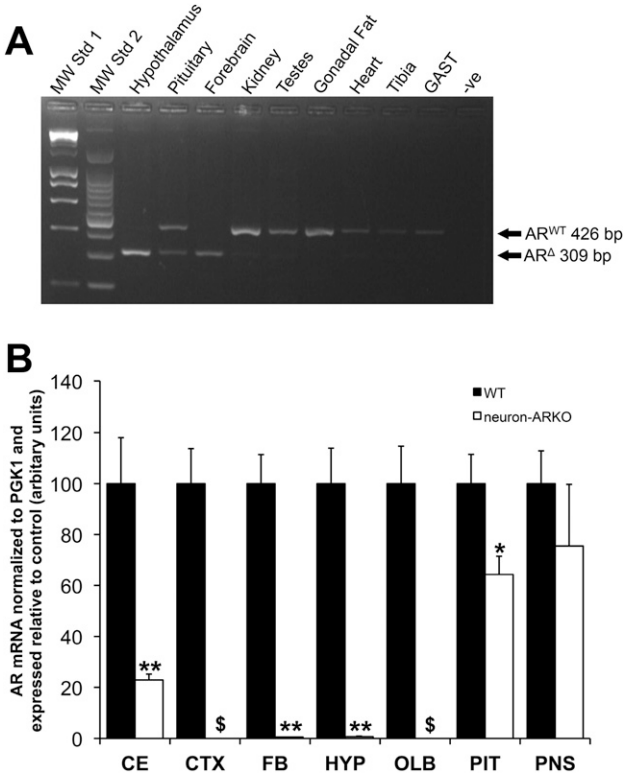

Figure 1. Characterization of Cre-mediated deletion of floxed AR allele in neuron-ARKO mice. (A) Representative image of reverse transcription PCR using cDNA isolated from various tissues of a neuron-ARKO male with AR-specific primers located in exons 2 and 4, WT AR: 426 bp, AR$^{\Delta ex3}$ in neuron-ARKOs: 309 bp; molecular weight standard (MW Std) 1: Hyperladder; MW Std 2: 100-bp ladder. (B) Quantitative real-time PCR analysis of AR mRNA in brain regions of neuron-ARKO males at 12 weeks of age. Values are mean + standard error of the mean; n = 7 to 13 per group except pituitary n = 5 per group; $ denotes undetectable levels of mRNA; *$P < 0.05$; **$P < 0.001$ *vs* WT. CE, cerebellum; CTX, cortex; FB, forebrain; HYP, hypothalamus; OLB, olfactory bulb; PIT, pituitary; PNS, peripheral nerves.

Downloaded from https://academic.oup.com/endo/article-abstract/158/10/3684/4056265 by Biomedical Library user on 04 April 2019

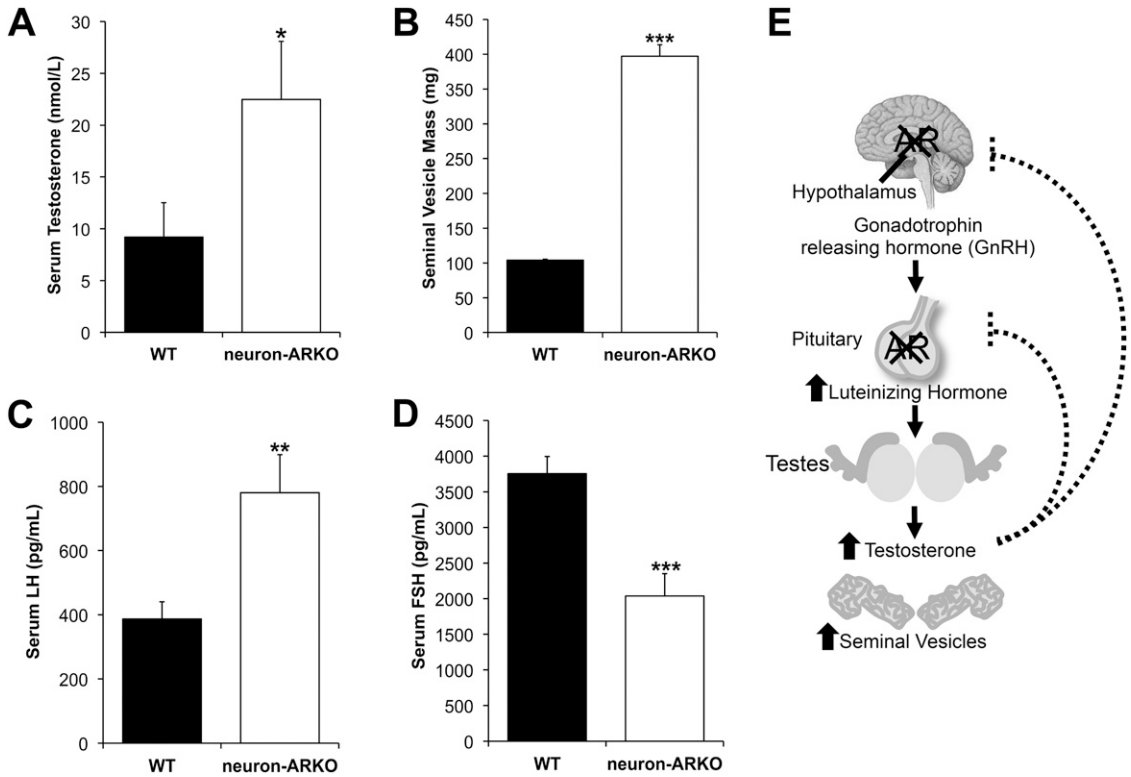

Figure 2. (A) Serum testosterone (nmol/L); (B) seminal vesicle mass (mg); (C) serum-luteinizing hormone (pg/mL); and (D) serum IGF-1 (ng/mL) at 12 weeks of age in WT and neuron-ARKO males. Values are mean + standard error of the mean; n = 7 to 13 per group; $*P < 0.05$; $**P < 0.01$; $***P < 0.001$ *vs* WT. (E) Disruption of the hypothalamic-pituitary-gonadal axis in neuron-ARKO males.

to a marked increase in the mass of the seminal vesicles by 380% compared with WT controls ($P < 0.001$) (Fig. 2B). In addition, there was an increase in the mass of the testes by 9% ($P < 0.05$) at 12 weeks of age and in kidney mass by 19% and 27% at 6 and 12 weeks of age, respectively ($P < 0.001$) (Table 2). The increased serum testosterone in neuron-ARKOs is most likely caused by disruption to the negative feedback of the hypothalamic-pituitary-gonadal axis as a result of AR deletion in the hypothalamus and pituitary (Fig. 2E). Consistent with this theory, we observed increased levels of serum LH in the neuron-ARKOs ($P < 0.01$) (Fig. 2C). Serum IGF-1 levels did not differ between WT and neuron-ARKO males at 12 weeks of age (Fig. 2D).

Table 2. Body Weight, Body Length, and the Mass of Various Tissues in Neuron-ARKOs and WT Littermate Controls at 6 and 12 Weeks of Age

Parameter	Age 6 Weeks		Age 12 Weeks	
	WT	Neuron-ARKO	WT	Neuron-ARKO
Body weight (mg)	22 ± 0.5	21 ± 0.4	26.9 ± 0.3	26.2 ± 0.3
Body length (mm)	83.4 ± 1.8	84.6 ± 1.1	91.9 ± 0.7	91.8 ± 0.7
Testis mass (mg)	78.3 ± 3.3	84.0 ± 2.6	101.3 ± 2.3	110.7 ± 2.6[a]
Levator ani mass (mg)	N/A	N/A	27.3 ± 1.7	32.2 ± 2.0
Kidney mass (mg)	154.8 ± 5.0	184.8 ± 5.7[b]	183.3 ± 2.7	232.5 ± 4.7[b]
Heart mass (mg)	133.8 ± 6.9	127.4 ± 3.6	158.3 ± 7.2	164.2 ± 7.8
Spleen mass (mg)	97.6 ± 11.0	98.2 ± 8.1	87.6 ± 5.4	87.5 ± 4.0
Subcutaneous fat mass (mg)	89.2 ± 6.0	80.4 ± 2.7	102.8 ± 6.6	88.1 ± 4.5
Renal fat mass (mg)	17.9 ± 1.7	14.4 ± 0.8	26.2 ± 4.4	20.0 ± 2.2
Gonadal fat mass (mg)	111.2 ± 11.0	112.7 ± 3.9	161.9 ± 13.5	158.9 ± 11.3
Brown adipose tissue mass (mg)	N/A	N/A	63.1 ± 3.2	58.5 ± 2.7

Values are mean ± standard error; n = 7 to 14 per group.

Abbreviation: N/A, not measured.

[a] $P < 0.05$ *vs* WT for same age group.

[b] $P < 0.001$ *vs* WT for same age group.

Downloaded from https://academic.oup.com/endo/article-abstract/158/10/3684/4056265 by Biomedical Library user on 04 April 2019

Neuron-ARKOs have decreased mass of fast-twitch hind-limb muscles

The body weight of the neuron-ARKOs did not differ from WT males at 6 or 12 weeks of age (Table 2). Despite the increase in serum testosterone in neuron-ARKOs, which we had predicted to increase hind-limb muscle mass, the mass of the Gast consisting of both fast-twitch and slow-twitch fibers was decreased by 11% ($P < 0.05$) and 13% ($P < 0.001$) in neuron-ARKOs compared with WT at 6 and 12 weeks of age, respectively. The mass of the EDL consisting predominantly of fast-twitch fibers was also decreased by 10% in neuron-ARKO males at 12 weeks of age ($P < 0.01$) (Fig. 3A and 3B). In contrast, the mass of the Sol, which consists of a high proportion of slow-twitch fibers, was unaffected in neuron-ARKOs (Fig. 3C). The decreased mass of the Gast hind-limb muscle in neuron-ARKOs was associated with a decrease in *Igf-1* gene expression ($P < 0.05$) (Fig. 3D) and an increase in protein expression of the mitochondrial CII-SDHB subunit ($P < 0.05$) (Fig. 3E; Supplemental Fig. 1). Although the mean protein levels of the mitochondrial subunits C1-NDUFBB8 and CV-ATP5A were

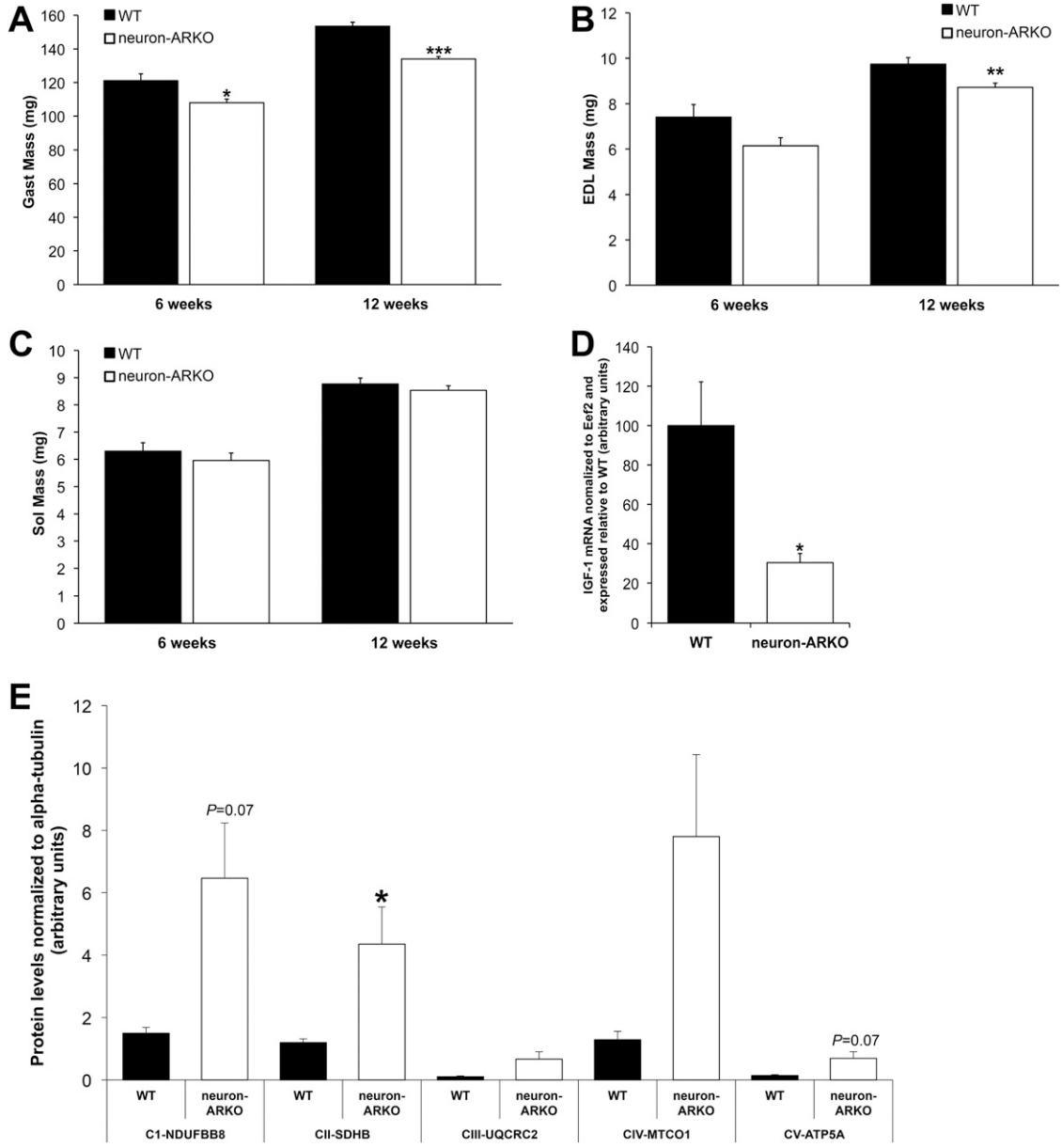

Figure 3. The mass of the hind-limb muscles. (A) The mixed-fiber Gast, (B) fast-twitch EDL, and (C) slow-twitch Sol at 6 and 12 weeks of age in WT and neuron-ARKO males. (D) *Igf-1* gene expression and (E) quantitation of protein expression of five oxidative phosphorylation (OXPHOS) mitochondrial complexes in Gast hind-limb muscle of WT and neuron-ARKOs at 12 weeks of age determined by Western blot analysis. Values are mean + standard error of the mean; n = 12 to 16 per group for hind-limb mass, n = 7 to 8 per group for mRNA, and n = 4 per group for Western blot analysis. *$P < 0.05$; **$P < 0.01$; ***$P < 0.001$ *vs* WT within age group.

Downloaded from https://academic.oup.com/endo/article-abstract/158/10/3684/4056265 by Biomedical Library user on 04 April 2019

higher in the Gast of neuron-ARKO compared with WT, this did not reach statistical significance ($P = 0.07$; Fig. 3E; Supplemental Fig. 1). The average size of the fast-twitch 2B fibers and the expression of *Tgfβ1* and the muscle genes *Myl3*, *MyH7*, *TnnI2*, *MyoD1*, and *MyH4* in Gast did not differ between WT and neuron-ARKO males (2B fiber size mean ± standard error, WT: 1129 ± 45 μm, neuron-ARKO: 925 ± 73 μm) (Supplemental Table 2).

Muscle strength is normal in the Gast hind-limb muscle of neuron-ARKOs

Average absolute force of the Gast muscle did not differ between WT and neuron-ARKO controls (Fig. 4A). As expected, average specific force was lower in the neuron-ARKOs compared with WT, but this did not reach statistical significance (mean ± standard error, WT: 204 ± 8 nM/mm^2, neuron-ARKO: 189 ± 8 mN/mm^2) (Fig. 4B). Following initiation of the fatigue protocol, both WT and neuron-ARKO mice exhibited decreased maximum force over time, with no significant difference observed between the WT and neuron-ARKOs (Fig. 4C). There was a significant time and genotype interaction with the maximum force of the neuron-ARKOs decreasing 0.13% faster than WT ($P < 0.001$). No differences in postfatigue force or following 10 minutes of recovery were observed between WT and neuron-ARKOs (Fig. 4C).

Physical activity is decreased in neuron-ARKO mice

Voluntary activity was unaffected in neuron-ARKO males at 6 weeks of age; however, it was decreased by 50% in neuron-ARKO males at 12 weeks of age compared with WT controls ($P < 0.05$) (Fig. 5A). Involuntary spontaneous physical activity was decreased by 27% ($P < 0.05$) and by 57% ($P < 0.01$) in neuron-ARKOs compared with WT at 6 and 12 weeks of age, respectively (Fig. 5B). Food intake was unaffected in neuron-ARKOs (Fig. 5C).

Discussion

It is paradoxical that exogenous testosterone clearly has anabolic effects on skeletal muscle mass in both humans and in mice, whereas data from several muscle-specific ARKOs, including our own targeting satellite cells, myocytes, myoblasts, and/or myofibers, provide no evidence for a direct role of androgens *via* the AR in skeletal muscle to regulate its mass (12–15). Evidence from these muscle-specific ARKO mouse models does, however, suggest a direct role for the AR in hind-limb muscles to regulate their force production (12, 14) and fiber-type distribution (15), whereas it is also a major determinant of the perineal muscle mass (12–15). In the current study, we have provided evidence for a role of the AR acting in neurons within the brain to positively regulate hind-limb muscle mass. We achieved this by generating a neuron-ARKO mouse model in which the AR is deleted specifically in neurons in the brain, including the hypothalamus, cortex, olfactory bulb, forebrain, cerebellum, and pituitary, as demonstrated by the lower AR mRNA levels in neuron-ARKOs compared with control littermates.

Deletion of the AR in these regions of the brain led to a twofold increase in serum testosterone and LH, most likely caused by disruption to the negative feedback of the hypothalamic-pituitary-gonadal axis as a result of AR deletion in the hypothalamus and pituitary. The rise in serum testosterone resulted in the predicted increase in the mass of the androgen-dependent organ, the seminal vesicles, in addition to the testes and kidneys. Similar disturbances to the hypothalamic-pituitary-gonadal axis have been observed in neruon-ARKOs generated using Nestin-Cre mice (18), consistent with the central actions of the AR playing a critical role in the negative feedback on LH secretion in the male (32). Interestingly, these neuron-ARKOs also displayed disruptions to the somatotropic axis evidenced by growth retardation and decreased serum levels of IGF-1 (18); however, these effects may be attributed to the reduced body length and serum growth hormone levels previously reported in Nestin-Cre

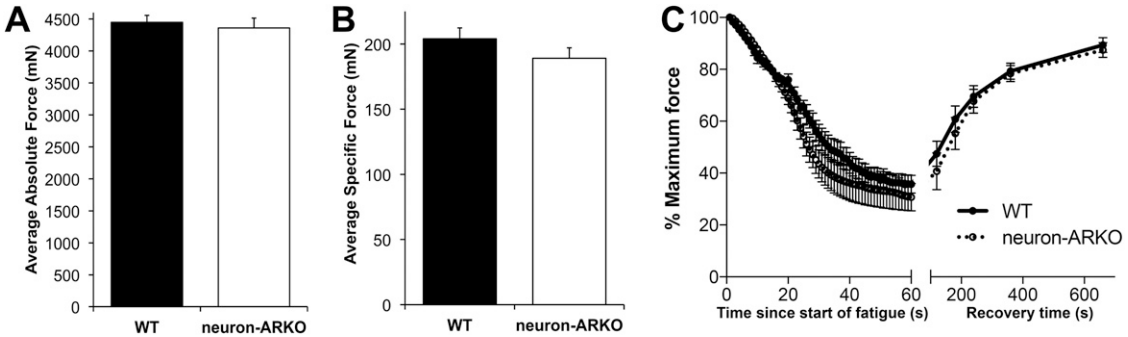

Figure 4. (A) Average absolute force; (B) average specific force; and (C) force-frequency test and recovery following fatigue of Gast muscle in WT and neuron-ARKO males at 10 weeks of age. Values are mean + standard error of the mean; n = 8 to 9 per group.

Downloaded from https://academic.oup.com/endo/article-abstract/158/10/3684/4056265 by Biomedical Library user on 04 April 2019

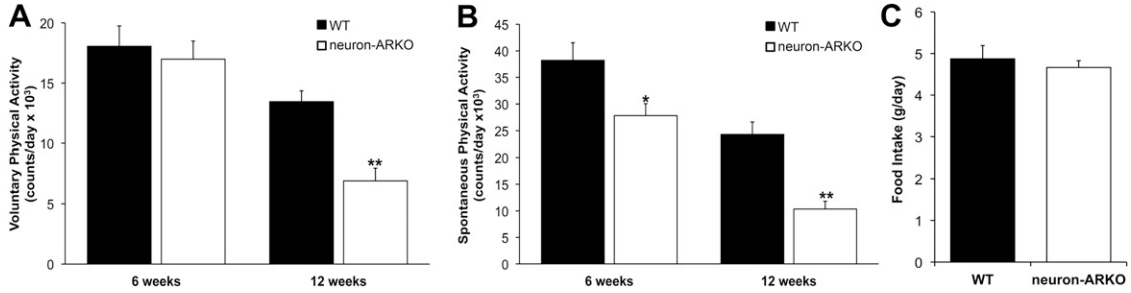

Figure 5. (A) Voluntary physical activity and (B) involuntary physical activity in WT and neuron-ARKO males at 6 and 12 weeks of age, and (C) food intake in WT and neuron-ARKO males at 12 weeks of age. Values are mean + standard error of the mean; n = 6 to 8 per group; $*P < 0.05$; $**P < 0.01$ *vs* WT.

mice (20) as neuron-ARKOs in the current study were of normal body length with normal serum IGF-1 levels.

The anabolic actions of testosterone to increase muscle mass in both men and male mice are well established (33, 34). Therefore, we predicted that the increase in circulating levels of testosterone in the neuron-ARKOs would increase hind-limb muscle mass. Surprisingly, however, the mass of the mixed fast- and slow-twitch hind-limb muscle Gast was decreased in neuron-ARKOs evident from 6 weeks of age. These data indicate an important role of the AR in neurons in Gast hind-limb muscle mass accrual during development. Reductions in the mass of the predominantly fast-twitch hind-limb muscle, EDL, were also observed in adult neuron-ARKOs at 12 weeks of age. In contrast, the predominantly slow-twitch fiber Sol muscle was unaffected in neuron-ARKOs, demonstrating a stimulatory action of androgens *via* the AR in neurons to increase the mass of fast-twitch hind-limb muscles. Given the numerous reports demonstrating a lack of effect of myocytic AR deletion in male mice on hind-limb muscle mass (12–15), these data suggest that the decrease in fast-twitch hind-limb muscle mass previously observed in the global-ARKO (9) and AR-null male mouse models (10, 11) is mediated, at least in part, by the loss of AR action in neurons within the brain.

A possible mechanism by which the AR exerts its anabolic effects on muscle mass accrual is *via* stimulation of the IGF-1/growth hormone axis. Neural deletion of the AR had no effect on the circulating levels of IGF-1, but decreased *Igf-1* gene expression within Gast of neuron-ARKOs. These data are consistent with the action of IGF-1 as a circulating hormone being distinct from its activity as an autocrine/paracrine growth factor (35). Whether the decreased *Igf-1* expression in Gast muscle is a direct result of neuronal AR deletion mediated *via* an efferent neural pathway or is secondary to its decreased mass remains to be determined. Previous observations of decreased *Igf-1* gene expression in atrophied Gast muscle of septic mice support the latter hypothesis (36). It is unlikely that the elevated testosterone in the neuron-ARKOs contributed to the decreased expression of *Igf-1* in the Gast, as previous studies report increased *Igf-1* expression in skeletal muscle cells following testosterone treatment both *in vitro* and *in vivo* (37, 38).

Reduced muscle mass and fiber size are inversely correlated with mitochondrial activity (39). To address the effect of the reduced fast-twitch hind-limb muscle mass in the neuron-ARKOs on mitochondrial activity, we determined the protein levels of five of the oxidative phosphorylation complexes. The Gast muscle of neuron-ARKOs contained a significantly higher level of the mitochondrial oxidative phosphorylation complex CII-SDHB with a trend for an increased in the complexes C1-NDIFBB8 and CV-ATP5A, indicative of increased mitochondrial activity. Because fiber size in the Gast of neuron-ARKOs was unaffected, this decrease in mitochondrial activity is most likely attributed to the increased serum testosterone levels in these mice, as testosterone treatment in male mice increases the expression of genes involved in mitochondrial biogenesis in skeletal muscle *via* an AR- dependent pathway (40).

The reduction in mass of the Gast hind-limb muscle in adult neuron-ARKOs at 12 weeks of age did not negatively impact on muscle strength as average absolute force and average specific force did not differ from WT controls. Following commencement of the fatigue protocol in the Gast, the maximum specific force in neuron-ARKOs decreased 0.13% faster than WT; however, as there was no difference in maximum specific force between neuron-ARKOs at any time point during the fatigue protocol or in their recovery postfatigue, these differences are unlikely to be physiologically relevant. Consistent with the lack of effect on muscle strength, transforming growth factor β1 mRNA levels in the Gast of neuron-ARKOs were unaffected (41). The average size of the fast-twitch 2B fibers and the expression of genes encoding the slow (*Myl3*, *MyH7*) and fast (*TnnI2*) muscle isoforms and those involved in muscle cell differentiation (*Myod1*) and muscle contraction (*MyH4*) were also unaffected in the Gast of neuron-ARKOs. These findings are consistent

Downloaded from https://academic.oup.com/endo/article-abstract/158/10/3684/4056265 by Biomedical Library user on 04 April 2019

with previous findings in muscle-specific ARKOs, demonstrating that the actions of testosterone to regulate muscle strength and fiber-type distribution are mediated directly *via* the AR in skeletal muscle (12–15), as this pathway of testosterone action remains intact in the neuron-ARKOs. In fact, this pathway of androgen action *via* the AR in skeletal muscle of neuron-ARKOs may be upregulated by their increased circulating testosterone, thereby aiding to maintain the strength of the fast-twitch hind-limb muscles despite their significantly decreased mass. It is also conceivable that the decrease in Gast mass of 13% in the neuron-ARKOs may not have been of sufficient magnitude to negatively impact on its strength.

It is well established that myocytic expression of the AR is the major determinant of the mass of the perineal muscles the LA and bulbocavernosus muscles (12–14). Consistent with these reports, the mass of the LA was unaffected in neuron-ARKOs compared with controls, indicating that the mass of the perineal muscles, unlike the hind-limb fast-twitch fiber muscles, is not regulated by the AR in neurons.

Voluntary and involuntary physical activity decreased by 50% and 65% in adult neuron-ARKOs compared with WT controls at 12 weeks of age. We have previously demonstrated a similar magnitude (70%) of decreased voluntary activity in global-ARKOs (42). Voluntary activity is also markedly reduced in AR-null males (10), whereas it is unaffected in muscle-ARKOs (13). These effects of the AR in neurons to positively regulate voluntary activity in male mice are likely to be independent of circulating testosterone levels, as, whereas voluntary activity is reduced by a similar magnitude in global-ARKOs and neuron-ARKOs, their respective serum testosterone levels are decreased and increased compared with controls (7). Involuntary activity in global-ARKOs, AR-null, or muscle-specific ARKO males has not been previously reported, and a contradictory observation of increased locomotor activity in neuron-ARKOs generated using Nestin-Cre mice has been described. It is difficult to make direct comparisons with the latter neuron-ARKO mouse, however, as Nestin-Cre mice themselves have a complicated metabolic phenotype (20, 21). The reduction in Gast muscle mass in neuron-ARKOs at 6 weeks of age coincides with the reduction observed in involuntary activity, whereas it precedes the decrease in voluntary activity that was not evident until 12 weeks of age. As such, it is therefore unlikely that the decrease in hind-limb muscle mass in neuron-ARKOs is due to decreased voluntary activity. Conversely, it is also feasible that the reduction in hind-limb muscle mass of the neuron-ARKOs decreased the motivation of the mice to voluntary exercise. We consider this unlikely given that muscle strength and resistance to fatigue of neuron-ARKOs did not differ from WT controls, and we have previously observed decreased voluntary activity in global-ARKO males compared with WT females (unpublished observation) despite their muscle mass and contractile strengths being similar (9). Our data in neuron-ARKOs provide strong evidence for a role of androgens acting *via* the AR in neurons within the brain to regulate voluntary activity. Studies using brain imaging by immunohistochemical detection of c-Fos in high-runner mice have identified several key regions of the brain associated with their increased motivation for running, including the prefrontal cortex, lateral hypothalamus, nucleus accumbens, and caudate-putamen, whereas activation of other regions of the brain, such as the hippocampus, is correlated with wheel running itself (43). It is well established that the AR is also expressed at many of these sites within the brain, with high levels of expression reported in the cortex, hippocampus, and hypothalamus (44). The precise region of the brain and the pathways responsible for mediating the inhibitory effects of the AR on voluntary and physical activity remains to be determined. These are likely to be complex, potentially involving a number of neural signaling networks such as dopamine and the endocannabinoid system in the control of voluntary activity and orexins in the control of involuntary activity, with brain reward centers being involved in both types of physical activity (45).

In conclusion, we have provided evidence for a role of androgen action *via* the AR in neurons in fast-twitch hind-limb muscle development and mass accrual in male mice. Muscle strength and fatigue were maintained in neuron-ARKOs most likely attributed to a direct action of testosterone on the AR in skeletal muscle, a pathway of testosterone action that remains intact in these mice. We also demonstrated that the AR in neurons within the brain acts to positively regulate voluntary and involuntary physical activity in males. The mechanism for these neural actions of the AR to regulate hind-limb mass and physical activity is unknown and requires further investigation using mouse models in which the AR has been deleted in specific regions and/or in a specific class of neurons within the brain. Understanding these central actions of androgens will provide a paradigm for the anabolic actions of androgens in muscle.

Acknowledgments

We thank Leonid Chuilov (Florey Institute, Melbourne, Victoria) for performing the random-effects generalized least squares regression analysis. The myosin heavy chain type IIB monoclonal antibody, developed by S. Schiaffino from the Universita degli Studi di Padova, and the α-tubulin monoclonal antibody,

Downloaded from https://academic.oup.com/endo/article-abstract/158/10/3684/4056265 by Biomedical Library user on 04 April 2019

developed by C. Walsh from the University of Pittsburgh, were obtained from the Developmental Studies Hybridoma Bank, created by the National Institute of Child Health and Human Development of the National Institutes of Health, and maintained at the University of Iowa Department of Biology, Iowa City, Iowa.

Financial Support: This work was supported by the Sir Edward Dunlop Medical Research Foundation (K.R.), the Austin Medical Research Foundation (R.A.D.), and a Les and Eva Erdi Research Grant (J.D.Z.). R.A.D. was supported by the National Health and Medical Research Council of Australia Project Grant APP1058189.

Correspondence and Reprint Requests: Rachel A. Davey, PhD, Department of Medicine, Austin Health, University of Melbourne, Studley Road, Heidelberg, Victoria 3084, Australia. E-mail: r.davey@unimelb.edu.au.

Disclosure Summary: The authors have nothing to disclose.

References

1. Bhasin S, Woodhouse L, Storer TW. Androgen effects on body composition. *Growth Horm IGF Res*. 2003;**13**(Suppl A):S63–S71.
2. Mauras N, Hayes V, Welch S, Rini A, Helgeson K, Dokler M, Veldhuis JD, Urban RJ. Testosterone deficiency in young men: marked alterations in whole body protein kinetics, strength, and adiposity. *J Clin Endocrinol Metab*. 1998;**83**(6):1886–1892.
3. Hamilton EJ, Gianatti E, Strauss BJ, Wentworth J, Lim-Joon D, Bolton D, Zajac JD, Grossmann M. Increase in visceral and subcutaneous abdominal fat in men with prostate cancer treated with androgen deprivation therapy. *Clin Endocrinol (Oxf)*. 2011;**74**(3):377–383.
4. Wang C, Swerdloff RS, Iranmanesh A, Dobs A, Snyder PJ, Cunningham G, Matsumoto AM, Weber T, Berman N; Testosterone Gel Study Group. Transdermal testosterone gel improves sexual function, mood, muscle strength, and body composition parameters in hypogonadal men. *J Clin Endocrinol Metab*. 2000;**85**(8):2839–2853.
5. Bhasin S, Storer TW, Berman N, Callegari C, Clevenger B, Phillips J, Bunnell TJ, Tricker R, Shirazi A, Casaburi R. The effects of supraphysiologic doses of testosterone on muscle size and strength in normal men. *N Engl J Med*. 1996;**335**(1):1–7.
6. Basaria S, Coviello AD, Travison TG, Storer TW, Farwell WR, Jette AM, Eder R, Tennstedt S, Ulloor J, Zhang A, Choong K, Lakshman KM, Mazer NA, Miciek R, Krasnoff J, Elmi A, Knapp PE, Brooks B, Appleman E, Aggarwal S, Bhasin G, Hede-Brierley L, Bhatia A, Collins L, LeBrasseur N, Fiore LD, Bhasin S. Adverse events associated with testosterone administration. *N Engl J Med*. 2010;**363**(2):109–122.
7. Notini AJ, Davey RA, McManus JF, Bate KL, Zajac JD. Genomic actions of the androgen receptor are required for normal male sexual differentiation in a mouse model. *J Mol Endocrinol*. 2005;**35**(3):547–555.
8. Pang TP, Clarke MV, Ghasem-Zadeh A, Lee NK, Davey RA, MacLean HE. A physiological role for androgen actions in the absence of androgen receptor DNA binding activity. *Mol Cell Endocrinol*. 2012;**348**(1):189–197.
9. MacLean HE, Chiu WS, Notini AJ, Axell AM, Davey RA, McManus JF, Ma C, Plant DR, Lynch GS, Zajac JD. Impaired skeletal muscle development and function in male, but not female, genomic androgen receptor knockout mice. *FASEB J*. 2008;**22**(8):2676–2689.
10. Ophoff J, Callewaert F, Venken K, De Gendt K, Ohlsson C, Gayan-Ramirez G, Decramer M, Boonen S, Bouillon R, Verhoeven G, Vanderschueren D. Physical activity in the androgen receptor knockout mouse: evidence for reversal of androgen deficiency on cancellous bone. *Biochem Biophys Res Commun*. 2009;**378**(1):139–144.
11. Altuwaijri S, Lee DK, Chuang KH, Ting HJ, Yang Z, Xu Q, Tsai MY, Yeh S, Hanchett LA, Chang HC, Chang C. Androgen receptor regulates expression of skeletal muscle-specific proteins and muscle cell types. *Endocrine*. 2004;**25**(1):27–32.
12. Dubois V, Laurent MR, Sinnesael M, Cielen N, Helsen C, Clinckemalie L, Spans L, Gayan-Ramirez G, Deldicque L, Hespel P, Carmeliet G, Vanderschueren D, Claessens F. A satellite cell-specific knockout of the androgen receptor reveals myostatin as a direct androgen target in skeletal muscle. *FASEB J*. 2014;**28**(7):2979–2994.
13. Rana K, Chiu MW, Russell PK, Skinner JP, Lee NK, Fam BC, Zajac JD, MacLean HE. Muscle-specific androgen receptor deletion shows limited actions in myoblasts but not in myofibers in different muscles in vivo. *J Mol Endocrinol*. 2016;**57**(2):125–138.
14. Chambon C, Duteil D, Vignaud A, Ferry A, Messaddeq N, Malivindi R, Kato S, Chambon P, Metzger D. Myocytic androgen receptor controls the strength but not the mass of limb muscles. *Proc Natl Acad Sci USA*. 2010;**107**(32):14327–14332.
15. Ophoff J, Van Proeyen K, Callewaert F, De Gendt K, De Bock K, Vanden Bosch A, Verhoeven G, Hespel P, Vanderschueren D. Androgen signaling in myocytes contributes to the maintenance of muscle mass and fiber type regulation but not to muscle strength or fatigue. *Endocrinology*. 2009;**150**(8):3558–3566.
16. Veldhuis JD, Anderson SM, Shah N, Bray M, Vick T, Gentili A, Mulligan T, Johnson ML, Weltman A, Evans WS, Iranmanesh A. Neurophysiological regulation and target-tissue impact of the pulsatile mode of growth hormone secretion in the human. *Growth Horm IGF Res*. 2001;**11**(Suppl A):S25–S37.
17. Lloyd CE, Palopoli M, Vary TC. Effect of central administration of interleukin-1 receptor antagonist on protein synthesis in skeletal muscle, kidney, and liver during sepsis. *Metabolism*. 2003;**52**(9):1218–1225.
18. Raskin K, de Gendt K, Duittoz A, Liere P, Verhoeven G, Tronche F, Mhaouty-Kodja S. Conditional inactivation of androgen receptor gene in the nervous system: effects on male behavioral and neuroendocrine responses. *J Neurosci*. 2009;**29**(14):4461–4470.
19. Yu IC, Lin HY, Liu NC, Sparks JD, Yeh S, Fang LY, Chen L, Chang C. Neuronal androgen receptor regulates insulin sensitivity via suppression of hypothalamic NF-κB-mediated PTP1B expression. *Diabetes*. 2013;**62**(2):411–423.
20. Harno E, Cottrell EC, White A. Metabolic pitfalls of CNS Cre-based technology. *Cell Metab*. 2013;**18**(1):21–28.
21. Declercq J, Brouwers B, Pruniau VP, Stijnen P, de Faudeur G, Tuand K, Meulemans S, Serneels L, Schraenen A, Schuit F, Creemers JW. Metabolic and behavioural phenotypes in nestin-Cre mice are caused by hypothalamic expression of human growth hormone. *PLoS One*. 2015;**10**(8):e0135502.
22. Casanova E, Fehsenfeld S, Mantamadiotis T, Lemberger T, Greiner E, Stewart AF, Schütz G. A CamKIIalpha iCre BAC allows brain-specific gene inactivation. *Genesis*. 2001;**31**(1):37–42.
23. Rana K, Clarke MV, Zajac JD, Davey RA, MacLean HE. Normal phenotype in conditional androgen receptor (AR) exon 3-floxed neomycin-negative male mice. *Endocr Res*. 2014;**39**(3):130–135.
24. Minichiello L, Korte M, Wolfer D, Kühn R, Unsicker K, Cestari V, Rossi-Arnaud C, Lipp HP, Bonhoeffer T, Klein R. Essential role for TrkB receptors in hippocampus-mediated learning. *Neuron*. 1999;**24**(2):401–414.
25. Funkat A, Massa CM, Jovanovska V, Proietto J, Andrikopoulos S. Metabolic adaptations of three inbred strains of mice (C57BL/6, DBA/2, and 129T2) in response to a high-fat diet. *J Nutr*. 2004;**134**(12):3264–3269.
26. MacLean HE, Chiu WS, Ma C, McManus JF, Davey RA, Cameron R, Notini AJ, Zajac JD. A floxed allele of the androgen receptor

Downloaded from https://academic.oup.com/endo/article-abstract/158/10/3684/4056265 by Biomedical Library user on 04 April 2019

gene causes hyperandrogenization in male mice. *Physiol Genomics*. 2008;**33**(1):133–137.
27. Davey RA, Hahn CN, May BK, Morris HA. Osteoblast gene expression in rat long bones: effects of ovariectomy and dihydrotestosterone on mRNA levels. *Calcif Tissue Int*. 2000;**67**(1): 75–79.
28. Boda E, Pini A, Hoxha E, Parolisi R, Tempia F. Selection of reference genes for quantitative real-time RT-PCR studies in mouse brain. *J Mol Neurosci*. 2009;**37**(3):238–253.
29. Kouadjo KE, Nishida Y, Cadrin-Girard JF, Yoshioka M, St-Amand J. Housekeeping and tissue-specific genes in mouse tissues. *BMC Genomics*. 2007;**8**:127.
30. Garton F, Seto JT, North KN, Yang N. Validation of an automated computational method for skeletal muscle fibre morphometry analysis. *Neuromuscul Disord*. 2010;**20**(8):540–547.
31. Banks GB, Judge LM, Allen JM, Chamberlain JS. The polyproline site in hinge 2 influences the functional capacity of truncated dystrophins. *PLoS Genet*. 2010;**6**(5):e1000958.
32. Wersinger SR, Haisenleder DJ, Lubahn DB, Rissman EF. Steroid feedback on gonadotropin release and pituitary gonadotropin subunit mRNA in mice lacking a functional estrogen receptor alpha. *Endocrine*. 1999;**11**(2):137–143.
33. Herbst KL, Bhasin S. Testosterone action on skeletal muscle. *Curr Opin Clin Nutr Metab Care*. 2004;**7**(3):271–277.
34. Axell AM, MacLean HE, Plant DR, Harcourt LJ, Davis JA, Jimenez M, Handelsman DJ, Lynch GS, Zajac JD. Continuous testosterone administration prevents skeletal muscle atrophy and enhances resistance to fatigue in orchidectomized male mice. *Am J Physiol Endocrinol Metab*. 2006;**291**(3):E506–E516.
35. Velloso CP. Regulation of muscle mass by growth hormone and IGF-I. *Br J Pharmacol*. 2008;**154**(3):557–568.
36. Nystrom G, Pruznak A, Huber D, Frost RA, Lang CH. Local insulin-like growth factor I prevents sepsis-induced muscle atrophy. *Metabolism*. 2009;**58**(6):787–797.
37. Serra C, Bhasin S, Tangherlini F, Barton ER, Ganno M, Zhang A, Shansky J, Vandenburgh HH, Travison TG, Jasuja R, Morris C. The role of GH and IGF-I in mediating anabolic effects of testosterone on androgen-responsive muscle. *Endocrinology*. 2011; **152**(1):193–206.
38. Lewis MI, Horvitz GD, Clemmons DR, Fournier M. Role of IGF-I and IGF-binding proteins within diaphragm muscle in modulating the effects of nandrolone. *Am J Physiol Endocrinol Metab*. 2002; **282**(2):E483–E490.
39. Schiaffino S, Reggiani C. Fiber types in mammalian skeletal muscles. *Physiol Rev*. 2011;**91**(4):1447–1531.
40. Usui T, Kajita K, Kajita T, Mori I, Hanamoto T, Ikeda T, Okada H, Taguchi K, Kitada Y, Morita H, Sasaki T, Kitamura T, Sato T, Kojima I, Ishizuka T. Elevated mitochondrial biogenesis in skeletal muscle is associated with testosterone-induced body weight loss in male mice. *FEBS Lett*. 2014;**588**(10):1935–1941.
41. Si Y, Kim S, Cui X, Zheng L, Oh SJ, Anderson T, AlSharabati M, Kazamel M, Volpicelli-Daley L, Bamman MM, Yu S, King PH. Transforming growth factor beta (TGF-β) is a muscle biomarker of disease progression in ALS and correlates with Smad expression. *PLoS One*. 2015;**10**(9):e0138425.
42. Rana K, Fam BC, Clarke MV, Pang TP, Zajac JD, MacLean HE. Increased adiposity in DNA binding-dependent androgen receptor knockout male mice associated with decreased voluntary activity and not insulin resistance. *Am J Physiol Endocrinol Metab*. 2011; **301**(5):E767–E778.
43. Rhodes JS, Gammie SC, Garland T, Jr. Neurobiology of mice selected for high voluntary wheel-running activity. *Integr Comp Biol*. 2005;**45**(3):438–455.
44. Dart DA, Waxman J, Aboagye EO, Bevan CL. Visualising androgen receptor activity in male and female mice. *PLoS One*. 2013; **8**(8):e71694.
45. Garland T, Jr, Schutz H, Chappell MA, Keeney BK, Meek TH, Copes LE, Acosta W, Drenowatz C, Maciel RC, van Dijk G, Kotz CM, Eisenmann JC. The biological control of voluntary exercise, spontaneous physical activity and daily energy expenditure in relation to obesity: human and rodent perspectives. *J Exp Biol*. 2011; **214**(Pt 2):206–229.

Downloaded from https://academic.oup.com/endo/article-abstract/158/10/3684/4056265 by Biomedical Library user on 04 April 2019